

5-2013

# QCM Aptasensor for Rapid and Specific Detection of Avian Influenza Virus

Luke Brockman

*University of Arkansas, Fayetteville*

Follow this and additional works at: <http://scholarworks.uark.edu/etd>

 Part of the [Pathogenic Microbiology Commons](#), [Pathology Commons](#), and the [Virology Commons](#)

---

## Recommended Citation

Brockman, Luke, "QCM Aptasensor for Rapid and Specific Detection of Avian Influenza Virus" (2013). *Theses and Dissertations*. 789.  
<http://scholarworks.uark.edu/etd/789>

This Thesis is brought to you for free and open access by ScholarWorks@UARK. It has been accepted for inclusion in Theses and Dissertations by an authorized administrator of ScholarWorks@UARK. For more information, please contact [scholar@uark.edu](mailto:scholar@uark.edu), [ccmiddle@uark.edu](mailto:ccmiddle@uark.edu).

## **QCM Aptasensor for Rapid and Specific Detection of Avian Influenza Virus**

# **QCM Aptasensor for Rapid and Specific Detection of Avian Influenza Virus**

A thesis submitted in partial fulfillment  
of the requirements for the degree of  
Master of Science in Biomedical Engineering

By

Luke David Brockman  
University of Arkansas  
Bachelor of Science in Biological Engineering, 2010

May 2013  
University of Arkansas

## **Abstract**

There has been a need for rapid detection of avian influenza virus (AIV) H5N1 due to it being a potential pandemic threat. Most of the current methods, including culture isolation and PCR, are very sensitive and specific but require specialized laboratories and trained personnel in order to complete the tests and are time-consuming. The goal of this study was to design a biosensor that would be able to rapidly detect AIV H5N1 using aptamers as biosensing material and a quartz crystal microbalance (QCM) for transducing method. Specific DNA aptamers against AIV H5N1 were immobilized, through biotin and streptavidin conjugation, onto the gold surface of QCM sensor to capture the target virus. Magnetic nanobeads (150 nm in diameter) were then added as amplifiers considering its large surface/volume ratio which allows for a higher target molecule binding rate and faster movement. The result showed that the captured AIV caused frequency change, and more change was observed when the AIV concentration increased. The nanobead amplification was effective at the lower concentrations of AIV; however, it was not significant when the AIV concentration was 1 HAU or higher. The detection limit of the aptasensor was 1 HAU with a detection time of 1 h. The capture of the target virus on to the surface of QCM sensor and the binding of magnetic nanobeads with the virus was confirmed with electron microscopy. Aptamers have unlimited shelf life and are temperature stable which allows this aptasensor to give much more consistent results specifically for in field applications.

**Keywords:** Aptasensor, Avian Influenza, QCM, Aptamer, Nanobeads

This thesis is approved for recommendation  
to the Graduate Council.

Thesis Director:

---

**Dr. Yanbin Li**

Thesis Committee:

---

**Dr. David Zaharoff**

---

**Dr. Michael Slavik**

## **Thesis Duplication Release**

I hereby authorize the University of Arkansas Libraries to duplicate this thesis when needed for research and/or scholarship.

**Agreed** \_\_\_\_\_  
**Luke David Brockman**

**Refused** \_\_\_\_\_  
**Luke David Brockman**

## **Acknowledgments**

First, I would like to thank my advisor, Dr. Yanbin Li, for his support throughout my Master's research. He was committed to helping me grow as a researcher which has been an extremely valuable experience. I have learned a lot by seeing first hand his passion for research.

Secondly, I would like to thank my committee members, Dr. Michael Slavik and Dr. David Zaharoff, for taking the time to review my Master's Thesis.

I would also like to thank Dr. Huaguang Lu of Penn State University for providing the non-target viruses used in my research.

I especially need to thank the research group for all of their support: Dr. Ronghui Wang for her help with all thing research related; Jacob Lum for being a great friend and also being there for me whenever I had questions or needed help in the Lab; Lisa Cooney for her help in SEM imaging; Dr. Yingchun Fu for sharing his knowledge of the QCM and analytical chemistry. I would also like to thank the rest of the research group for their friendship and support.

I would like to thank the Department of Biomedical Engineering for supporting me throughout my Master's program and the Department of Biological and Agricultural Engineering for supporting me with a teaching assistantship throughout my graduate studies.

This research was supported in part by the Arkansas Biosciences Institute and they are greatly appreciated for their financial support.

Lastly, and most importantly, I would like to thank my parents for everything they have done for me. They have always been supportive of whatever I chose to do and I can't thank them

enough for that. Their love and support is what made it possible for me to achieve my academic goals and I can't put in to words how much they have meant to me.



## Table of Contents

<b>Chapter 1 Introduction.....</b>	<b>1</b>
<b>Chapter 2 Objectives.....</b>	<b>4</b>
<b>Chapter 3 Review of Literature.....</b>	<b>6</b>
3.1 H5N1 Influenza Virus.....	7
3.2 Current Detection Methods for H5N1.....	9
3.3 Biosensors.....	10
3.3.1 Major Types of Biosensors used in Microbial Detection.....	11
3.3.2 Biosensors for Detection of Avian Influenza.....	13
3.3.3 Quartz Crystal Microbalance Biosensors.....	14
3.3.4 Aptamers.....	16
3.3.5 Electrode Modification in QCM Biosensors.....	17
3.4 Magnetic Nanoparticles.....	18
<b>Chapter 4 Materials and Methods.....</b>	<b>19</b>
4.1 Materials.....	20
4.1.1 Biological and Chemical Reagents.....	20
4.1.2 Virus and Aptamers.....	20
4.1.3 Instruments and Electrodes.....	21
4.2 Detection of AIV H5N1.....	23
4.2.1 Pretreatment of Electrodes.....	23
4.2.2 Preparation of 150 nm Magnetic Nanobeads.....	23
4.2.3 Detection of AIV H5N1.....	24
4.2.4 Specificity Tests.....	26
4.2.5 Data Analysis.....	26
4.3 Calculation of Captured Virus.....	27

<b>Chapter 5 Results and Discussion.....</b>	<b>28</b>
5.1 Fabrication and Characterization of the QCM Aptasensor.....	29
5.2 Detection of AIV H5N1.....	31
5.3 Specificity of the Aptasensor.....	36
<b>Chapter 6 Conclusions.....</b>	<b>38</b>
<b>Chapter 7 Recommendations for Future Research.....</b>	<b>40</b>
<b>References.....</b>	<b>42</b>

## List of Tables

<b>Table 5.1</b> Frequency values of the QCM aptasensor for each titer (HAU) of AI H5N1 virus in PBS solution. Error values indicate the standard deviation (n=3).....	32
<b>Table 5.2</b> Comparison of calculated virus captured versus the number of virus added.....	33
<b>Table 5.3</b> Comparison of treatment means. Levels not connected by the same letter are not significantly different.....	34
<b>Table 5.4</b> P values for each H5N1 concentration determining the significance of nanobead amplification. P values greater than .05 are considered not significantly different. ....	34

## List of Figures

<b>Figure 4.1</b> H5N1 aptamer secondary structure.....	21
<b>Figure 4.2</b> Schematic of the aptasensor. The biological sensing element is immobilized on the electrode surface. The quartz in the electrode acts as a transducer, converting the mass change to a frequency signal. The QCM processes and records all of the data.....	22
<b>Figure 4.3</b> Instruments and electrodes. (a) QCA 922 quartz crystal analyzer. (b) 8 MHz AT-cut quartz crystal electrode. (c) 70 $\mu$ l acrylic flow cell.....	22
<b>Figure 4.4</b> Functionalization of streptavidin coated 150 nm magnetic nanobeads with biotinylated aptamer against H5N1.....	24
<b>Figure 4.5</b> The electrode modification, virus detection and signal amplification of the aptasensor. a) Streptavidin adsorption; b) aptamer immobilization by streptavidin binding; c) PEG blocking of unbound sites; d) capturing of target H5N1 virus; e) amplification by nanobead labeling.....	25
<b>Figure 5.1</b> Frequency shifts of the QCM aptasensor comparing BSA and PEG blocking agents for AIV H5N1.....	30
<b>Figure 5.2</b> Typical sensorgram of the QCM aptasensor for surface modification, aptamer immobilization, target AIV detection and signal amplification with nanobeads. The concentration of AIV H5N1 was 1 HA in this test.....	31
<b>Figure 5.3</b> Frequency shifts of the QCM aptasensor as a function of the titer (HAU) of AI H5N1 virus in PBS solution. The detection limit is determined as 1 HAU. Error bars indicate the standard deviation (n=3).....	32

**Figure 5.4** SEM image of the top view of the QCM surface. Confirmation of the binding of a magnetic nanobead with a 150 nm diameter to a target H5N1 virus (80 nm diameter).....36

**Figure 5.5** Frequency shifts of the QCM aptasensor for the target AIV H5N1 virus along with the five non-target AIV subtypes at 2 HAU. Error bars indicate standard deviation (n=3).....37

## **Chapter 1 Introduction**

Avian influenza viruses (AIV) are a genus of virus in the family *Orthomyxoviridae* consisting of a single stranded negative sense RNA genome segmented into eight fragments (Lee & Saif, 2009). They can occur in both low pathogenic and high pathogenic strains. Two types of antigen proteins are found on the surface of the virus, hemagglutinin (HA) and neuraminidase (NA), which determine the subtype of the virus. High pathogenic avian influenza subtype H5N1 mainly affects birds but in rare cases humans can become infected after close, direct contact with infected birds (Fang et al., 2008). It was first discovered in humans in 1997 in Hong Kong. Since then the virus has spread throughout much of south Asia and parts of Europe and Africa. The virus often has a mortality rate of 100% in poultry while having a 60% mortality rate in humans. Since 2003, there have been a total of 622 reported cases in humans resulting in 371 deaths (WHO, 2013). It is estimated that H5N1 has already cost the poultry industry over \$10 billion and the World Bank has estimated that a severe human outbreak would cost upwards of \$3 trillion to the global economy (Burns et al., 2008). For these reasons, it is extremely important to have rapid detection of AIV H5N1 to prevent outbreaks. The current gold standard for avian influenza detection are viral isolation cultures and real-time RT-PCR. They both provide high sensitivity but are time consuming, expensive, and require special training and facilities (Charlton et al., 2009; Ellis & Zambon, 2002). These longer tests may allow the virus to spread which is why more reliable, rapid detection methods are needed.

As an alternative, biosensors have been studied for the detection of avian influenza virus. Biosensors, which combine a biological sensing element, a transducer, and a signal processing unit, have shown a lot of promise for rapid detection of virus (Amano & Cheng, 2005). Quartz crystal microbalance (QCM) has gained popularity due to its simplicity and cost effectiveness (Ivnitski et al., 1999). The QCM biosensor is based on the piezoelectric properties of a quartz

crystal wafer when an electric field is applied across the electrodes. The change in resonant frequency can be attributed to a change in mass on the electrode surface. Many biological sensing elements have been used with biosensors, but aptamers are becoming more popular due to their stability and ease of manipulation.

In this research, a previously developed aptamer against AIV H5N1 was used with the QCM biosensor along with nanobead amplification. The objective was to improve specificity, decrease the lower detection limit and reduce the detection time for AIV H5N1.



## **Chapter 2 Objectives**

Avian influenza H5N1 is a highly pathogenic virus that has the potential to have major health and economic impacts. Current detection methods either lack specificity or are too time consuming and expensive to be used for rapid, on-site testing. The QCM biosensor has been developed to meet these goals but is currently lacking the sensitivity required. The objective of this study was to improve the specificity and sensitivity of the biosensor by using an aptamer against AIV H5N1, rather than the traditional antibody, as well as nanobead amplification to further increase the sensitivity.

The specific objectives of this project were as follows:

1. To determine the effectiveness of using an aptamer as an alternative biological recognition element for improving the specificity and sensitivity of the biosensor for H5N1.
2. To determine the effectiveness of using aptamer labeled nanobeads as mass amplifiers to further lower the detection limit of the AIV H5N1 biosensor.

## **Chapter 3    Review of the Literature**

### 3.1 H5N1 Influenza virus

Influenza A viruses are a genus of virus in the family *Orthomyxoviridae* consisting of a single stranded negative sense RNA genome segmented into 8 fragments (Lee & Saif, 2009). The structure of the virus is a helical capsid surrounded by a lipoprotein envelope. For the virus to be infectious a functional copy of each genome segment must be present. The nucleocapsid is covered by a lipoprotein membrane which consists of a lipid layer interspersed with membrane proteins. The lipoprotein envelope of *Orthomyxoviridae* viruses can occur in either spherical or helical forms with the shape being dependent on its surface proteins (Jin et al., 1997). Spherical virus particles are typically 50-120 nm in diameter, while filamentous particles typically have a diameter around 20 nm and a length of 200-300 nm.

Two types of antigen proteins are found on the surface of the virus, hemagglutinin (HA) and neuraminidase (NA). Each virus particle contains 500-1000 hemagglutinin proteins and 100-500 neuraminidase proteins (Mitnaul et al., 2000). The virus subtype is determined by the specific type of hemagglutinin and neuraminidase present on the surface. In total there are 16 different HA subtypes and 9 NA subtypes.

The natural host of influenza A particles are wild birds, primarily water fowl. These can carry and shed virus even while showing no outward symptoms. The primary virus transmission route is fecal-oral in birds while mammals transmit infection more through respiratory. Though the virus can be stable up to a week in the environment, the presence of a lipoprotein envelope makes the virus particles susceptible to deactivation by disinfectants and detergents (Harder & Werner, 2006).

High pathogenic avian influenza subtype H5N1 mainly affects birds but in rare cases humans can become infected after close, direct contact with infected birds (Fang et al., 2008). The high pathogenic strain of H5N1 was first isolated from a farm goose in Guangdong parish of China in 1996. In 1997 the first known human case occurred in Hong Kong when 18 people became infected, resulting in 6 deaths. Since 2003, there have been a total of 622 reported cases in humans resulting in 371 deaths (WHO, 2013). It is estimated that H5N1 has already cost the poultry industry over \$10 billion and the World Bank has estimated that a severe human outbreak would cost upwards of \$3 trillion to the global economy (Burns et al., 2008). So far there is very little evidence of human to human transmission but there is always the danger that H5N1 will gain a mutation which would allow for efficient transmission between humans (Li et al., 2004).

The difference between the high pathogenic and low pathogenic strains of H5N1 can be attributed to the ease of which the H5-variant of the HA protein can be cleaved. The cleavage site of high pathogenic H5N1 contains a large number of basic amino acid residues allowing it to be cleaved by a variety of host proteases. This allows the virus to be able to infect more of the body outside the respiratory tract (Steinhaeur, 1999).

In birds typical symptoms of H5N1 include swelling of the head and neck region, reduced egg production, decreased food and water consumption, ruffled feathers, conjunctivitis, and throat and nasal discharge. High pathogenic H5N1 has a high mortality rate of between 90-100% in domestic birds (Boyce et al., 2009). Symptoms in humans are similar to those of the common flu but are much more severe and include fever, cough, sore throat, muscle aches, conjunctivitis, and sometimes even pneumonia (Hien et al., 2009). It is estimated that many mild

cases of H5N1 go unreported which would therefore cause the reported mortality rate of 60% in humans to be lower (Thorson et al., 2006).

### **3.2 Current Detection Methods for H5N1**

An avian influenza virus outbreak would have huge economic impacts on top of the potential loss of human life. Poultry industries would be crippled not only by the loss of their flock but also from the time it would take to quarantine the infected birds to prevent further spread (Burns et al., 2008). For these reasons, it is essential to have reliable, rapid detection methods for reducing the spread of avian influenza. Some of the current detection methods for avian influenza include viral isolation culture, immunochromatographic strips, direct immunofluorescent assay, enzyme-linked immunoassay, hemagglutinin-inhibition, and reverse-transcription-polymerase chain reaction (Amano & Cheng, 2005).

The gold standard method for which all virus detection methods are compared is the viral isolation culture with immunological antigen conformation (Leland & Ginocchico, 2007). For viral isolation specific pathogen free embryonated chicken eggs or cell cultures must first be inoculated with the virus sample. Doing this allows the virus infectivity to be measured in either 50% Egg Infectious Dose per ml (EID<sub>50</sub>/ml) or 50% Tissue Culture Infectious Dose per ml (TCID<sub>50</sub>/ml). Following this technique, hemagglutinin inhibition is performed for subtyping of the virus. First antisera must be isolated from an infected bird and then serially diluted. This is then added to a standard HA concentration of different virus subtypes along with erythrocytes. Antibody binding will hinder the agglutination of erythrocytes, thus identifying the subtype of virus. Although viral isolation provides great sensitivity and is inexpensive in comparison to other methods, its requirement of long incubation times, high technical expertise, specialized

eggs or cell cultures, and live viruses prevents it from being an efficient detection method (Charlton et al., 2009).

A lot of the disadvantages of cell culture techniques, such as long incubation times and high expertise requirements, have been overcome by molecular detection methods. One molecular detection method that offers fast detection times and high sensitivity is reverse transcription-polymerase chain reaction (RT-PCR). Because avian influenza has a RNA genome reverse transcriptase must be used to convert the genome to DNA copies (cDNA) for use in PCR. The cDNA segments are then further amplified by the enzyme polymerase. DNA primers are used to serve as a starting point for DNA replication and can also be used for the detection of a specific avian influenza gene (Dawson et al., 2007). Other methods for detection of H5N1 include the use of real time RT-PCR. It is based on the RT-PCR method but uses fluorescent probes to detect specific gene fragments at the same time as gene amplification. These probes are specific to the desired sequence of DNA which makes the real time RT-PCR method much more specific than the traditional RT-PCR. In addition to increased specificity, real time RT-PCR also has the capability of using multiple probes to detect multiple genes simultaneously. RT-PCR methods are still the gold standard for rapid tests because of their sensitivity and specificity but they still have the disadvantage of being expensive, having high false positive rates, requiring specialized laboratories and equipment, and consist of a complicated procedure which requires extensive training (Ellis & Zambon, 2002).

Immunochromatographic strips are a very simple detection method which use enzyme-labeled anti-nucleoprotein antibodies bound to a membrane and reagents to cause a color change on a strip signifying the presence of virus. These tests can be completed in less than 30 min and

are very easy to perform. The downside is that they do not provide any subtype information for the virus and have low sensitivity requiring follow up testing in most situations (Marandi, 2010).

### **3.3 Biosensors**

A biosensor consists of three parts: biological element, transducing element, and a signal processing element. The biosensor uses the biological element as a functional group which may be an enzyme, antibody, protein, cell, virus, organelle or aptamer. This recognition element's interaction with the target analyte causes a biochemical change in the environment that the transducing element can detect through mechanical, electrochemical, piezoelectric, optical or thermal measurements (Nayak et al, 2009). The signal from the transducer is then converted by the processing element to produce useable data.

Biosensor research first began in the 1960s when Clark and Lyons proposed the first glucose sensor at Children's Hospital in Cincinnati. Since then, biosensors applications have expanded throughout the medical field as well as agriculture, food safety, environmental protection, biodefense and many others (Wang, 2001). Biosensors offer many advantages over conventional methods including targeted specificity, fast response times, continuous data collection and simplified sample preparation (Deisingh & Thompson, 2004).

#### **3.3.1 Major Types of Biosensors used in Microbial Detection**

As previously mentioned there are now many types of biosensors but two main types have been studied for microbial detection: electrochemical and optical.

Electrochemical biosensors measure the changes in the electrical properties caused by biochemical reactions to detect an analyte (Grieshaber et al., 2008). They offer many advantages



including low cost, ease of miniaturization and low power costs (Pejcic et al., 2006). There are four main types of electrochemical biosensors: amperometric, potentiometric, conductimetric, and impedimetric. Amperometric biosensors apply a constant potential across an electrode and measure the current associated with either the reduction or oxidation of an electroactive species created by its interaction with the biological element (Lojou & Bianco, 2006). Potentiometric biosensors convert the biological reaction into a potential signal by using ion-selective electrodes (Konki, 2007). Conductimetric biosensors simply measure the conductivity change caused by the analytes. Impedance or impedimetric biosensors are a class of electrochemical biosensors which measure a combination of the resistive and capacitive or inductive properties of a material in response to a small amplitude sinusoidal excitation signal (Varshney & Li, 2009).

Electrochemical biosensors have been extensively researched for the detection of cells, bacteria, viruses, proteins and chemicals. They have made major advances in the areas of point-of-care cancer diagnosis, cancer-related proteins and specific mutations in DNA (Wang, 2006). Food safety is also another popular field for the use of electrochemical biosensors. They have been used to detect the presence of antibiotics in milk products down to 2.6 ng/ml (Davis & Higson, 2010). There are numerous impedance biosensors that have been shown to be able to detect bacteria and viruses (Varshney & Li, 2009; Wang et al., 2009; Lum et al., 2012; Bai et al., 2012). Finally, the most common electrochemical sensor today is the glucose sensor which is used by millions of diabetics on a daily basis (Wang, 2008).

Optical biosensors use visual phenomenon to detect any interaction between the sensing element and the analyte. Examples of these sensors include surface plasmon resonance (SPR), absorption, luminescence and fluorescence sensors. These biosensors can work in multiple ways: the binding of the analyte can directly affect the optical properties of the environment, such as in

SPR or absorption, or the analyte can be tagged with a label that produces an optical phenomenon, such as fluorescence.

Fluorescence is one of the most commonly studied types of optical sensors and they typically use dyes, quantum dots and fluorescent proteins as labels (Medintz et al., 2005). Because quantum dots have a narrow excitation wavelength they have been successfully used to simultaneously detect separate pathogens (Yang & Li, 2006). A green fluorescence protein gene has also been successfully inserted into *Listeria monocytogenes* for the detection of bacteria inside of cells (Fortineau et al., 2000).

Label-free optical biosensors are able to avoid some of the disadvantages of fluorescent labels, such as false positives and negatives and requiring an extra step (Cooper, 2002). SPR biosensors measure the refractive index of the electrode surface which changes with the addition of biomolecules. The SPR has proven to be effective in the detection of bacteria, viruses and proteins in real time (Phillips & Cheng, 2007). It has also been used to quantify influenza virus for vaccine production using an antibody inhibition assay on the sensor surface (Estmer-Nilsson et al., 2008).

### **3.3.2 Biosensors for Detection of Avian Influenza**

Since the global outbreak of avian influenza, there has been a large emphasis for developing biosensors for the detection of the avian influenza virus. Bai et al. (2012) was able to use an SPR aptasensor to detect H5N1 from swab samples all the way down to 0.128 HAU. Chang et al. (2010) developed a surface plasmon fluorescence fiber-optic biosensor to detect H1N1 down to 13.9 pg/ml. A fluorescence biosensor using CdTe quantum dots was developed by Nguyen et al. (2012) to successfully detect 3 ng/ $\mu$ l of H5N1 virus. Xu et al. (2007) developed

an optical interferometry biosensor to capture influenza subtypes H7 and H8 using antibodies with detection limits as low as 0.0005 hemagglutination units per milliliter. Electrically active magnetic nanoparticles were used by Kamikawa et al. (2010) in their electrochemical biosensor to detect H5N1 at 1.4  $\mu\text{M}$ . Lastly, Lum et al. (2012) developed an impedance biosensor with red blood cell amplification for H5N1 with a detection limit of  $10^3$  EID<sub>50</sub>/ml. These developed sensors have shown potential but are not suitable for rapid, in-field testing due to either their lack of specificity, are too time-consuming, or are not practical for use on site.

### 3.3.3 Quartz Crystal Microbalance Biosensors

Quartz crystal microbalance (QCM) has been gaining popularity due to its simplicity and cost effectiveness (Ivnitski et al., 1999). The QCM biosensor is based on the piezoelectric properties of a quartz crystal wafer. This effect was first discovered in 1880 by Pierre and Jacques Curie after noticing that an application of voltage across quartz caused physical displacements. In the sensors early stages its simplicity and sensitivity allowed it to consistently detect mass in a vacuum within 2% of its true value (Lu & Czanderna, 1984). For the modern QCM biosensor a quartz wafer is sandwiched between two excitation electrodes which apply an electric field across the wafer. This creates an inverse piezoelectric effect, causing deformation of the crystal. The change of the resonant frequency of the crystal is attributed to a change in mass on the electrode surface (Bard & Faulkner, 2001). For gas-phase measurement, the relationship between the frequency change ( $\Delta f$ ) and mass change ( $\Delta m$ ) of the crystal is expressed by the Sauerbrey equation (Sauerbrey, 1959):

$$\Delta f = -C_f(f_0)^2 \left( \frac{\Delta m}{A} \right) \quad 3.1$$

where  $A$  is the electrode area,  $f_0$  is the resonant frequency and  $C_f$  is the sensitivity factor for the crystal. More recently the sensor has evolved to be able to measure mass in liquid media as well. For liquid-phase measurement, a most commonly used model was by Kanazawa and Gordon (1985) as follows (Vogt et al., 2004):

$$\Delta f = \frac{-\sqrt{f_{ro}\rho_l\eta_{lm}}}{\rho_q h\sqrt{2\pi}} \sin\left[\frac{\pi}{4} - \frac{\phi_l}{2}\right] \quad 3.2$$

where  $h$  is the thickness of the quartz crystal,  $\rho_q$  is the density of the quartz,  $f_{ro}$  is the resonance frequency of the unloaded resonator, and  $\rho_l$ ,  $\eta_{lm}$ , and  $\phi_l$  are density, magnitude of the complex viscosity, and relative phase angle of the liquid medium, respectively. The combination of equations 3.1 and 3.2 can describe the behavior of biological applications in liquid media. While rapid and easy to use, the QCM biosensor still lacks the sensitivity needed to be considered an effective detection method for avian influenza virus.

QCM biosensors have been well studied for the detection of bacteria, viruses, cells, proteins and nucleic acids. Other techniques are often coupled with QCM to increase the performance and capability of the biosensor. Liu et al. (2007) used the QCM to detect *E. coli* O157:H7 at  $10^2$  cfu/ml while also comparing different nanobead sizes for amplification. Magnetic separation in combination with the QCM has shown to be effective in demonstrating the feasibility of QCM as an on-line detection technique (Tsai et al., 2008).

There have been a few previous studies using the QCM to rapidly detect AIV. Perduru Hewa et al. (2009) were able to use the QCM to detect influenza virus in nasal washings with a lower detection limit of  $10^4$  plaque forming units/ml (pfu/ml). With the addition of gold nanoparticles they were able to further reduce the detection limit down to  $10^3$  pfu/ml which is

comparable to the sensitivity of viral isolation techniques. However, this was only able to detect influenza A virus with no subtype information. Li et al. (2011) was able to successfully detect H5N1 using antibodies and nanobead amplification down to 1 HAU with a detection time of 2 h. Owen et al. (2007) used aerosolized influenza virus with the QCM and successfully detected down to 4 virus particles/ml in a gas media. Most recently, Wang & Li (2013) developed a hydrogel based QCM aptasensor to greatly reduce their detection limit down to 0.0128 HAU. Improvements can still be made not only in the sensitivity and specificity of these tests but in the detection time and simplicity of the tests as well. Traditionally the QCM immunosensors have been developed for bacteria and virus detection but the emergence of aptamers has led to more alternatives in QCM biosensor research.

### **3.3.4 Aptamers**

The ability to create recognition molecules with specific properties is ideal for use in biosensor research. Because of this much time and effort has been put in to the molecular engineering of oligonucleotides due to their ease of design. This can be done with extreme accuracy, thus there is little or no batch to batch variation in their production (Sefah et al., 2009). Therefore, aptamers can offer a strong and reliable alternative as a biological element in many biosensing applications. Aptamers are artificially created single-stranded oligonucleotides that have the ability to bind to targets such as amino acids, drugs, proteins, cells, and viruses with high affinity and specificity (Jayasena, 1999). They are selected through an in vitro process from random oligonucleotide pools called Systematic Evolution of Ligands by EXponential enrichment (SELEX). Simply put, this involves the combination of an oligonucleotide library with the target molecule. After washing, the bound sequences are amplified by PCR and the process is repeated again until the pool is enriched with oligonucleotide strands that are specific

to only the target (Tuerk & Gold, 1990; Ellington & Szostak, 1990). This allows aptamers to be generated against a wide variety of targets and this list will continue to grow as technology and research expands. Aptamers show a very high affinity to their targets, comparable to those of monoclonal antibodies (Jenison et al., 1994). Aptamers can provide a number of advantages over antibodies, namely the ease at which they are designed and modified, higher thermal stability, no batch to batch variation and a much longer shelf life (Sefah et al., 2009). In addition, the small size and uniformity of aptamers is especially important for the QCM as it allows the captured mass to be closer to the electrode surface, providing lower noise and higher repeatability.

These great properties of aptamers have allowed them to be implemented in many different fields of, such as bio-technology, medicine, pharmacology, cell biology, microbiology, and analytical chemistry to name a few (Mascini, 2009). They have also been considered by researchers to improve the sensitivity and specificity of QCM biosensors. Bai et al. (2012) used an aptamer based SPR biosensor for the detection of AIV H5N1 and successfully detected down to 0.128 HAU. As previously mentioned, Wang and Li (2013) developed a hydrogel based QCM aptasensor for the detection of AIV H5N1. Cui et al. (2011) was able to use aptamers specifically as a labeling technique for quantum dots against Influenza A particles.

### **3.3.5 Electrode Modification in QCM Biosensors**

Because the QCM relies on detecting changes in mass by the capturing of targets by a recognition molecule, it is important that the recognition elements are not only securely immobilized on the electrode but properly arranged to have the highest possibly capture efficiency as well. To do this it is necessary to choose an immobilization method that preserves the aptamer affinity, controls their orientation and minimizes their interference with the

capturing of the target. For aptamers there are only two main immobilization techniques. Self-assembled monolayers (SAMs) can be created by submersing the electrode in a thiol buffer solution. After rinsing, the addition of aptamers with an amine group attached will then become immobilized on the surface. Aptamers can also be immobilized on the gold surface through biocoating. Avidin (or one of its derivatives) can easily coat the gold electrode surface through physisorption. Biotin conjugated aptamers are then immobilized on the electrode through the biotin-avidin conjugation (Balamurugan et al., 2007). Because SAMs are time consuming and potentially less effective, the biocoating technique seems more efficient.

### **3.3.6 Magnetic Nanoparticles**

Magnetic nanoparticles are defined as a paramagnetic material with at least one dimension ranging in the size of 1-100 nm. Magnetic nanobeads are widely used for biosensors not only for signal amplification but separation as well due to their strong magnetic properties and low toxicity (Hewa et al., 2009; Li et al, 2011; Lum et al., 2012). Magnetic nanobeads have several advantages in biosensing applications over the previously used microbeads. They have a larger surface/volume ratio allowing for faster movement and high target molecule binding rate (Hsing et al., 2006).

## **Chapter 4    Materials and Methods**



## **4.1 Materials**

### **4.1.1 Biological and Chemical Reagents**

Phosphate buffered saline (PBS, 10X) was purchased from Sigma-Aldrich (St. Louis, MO) and diluted with Milli-Q (Milli-Q, Bedford, MA) water to 10 mM (pH 7.4) for use in all tests. Poly (ethylene glycol) methyl ether thiol (PEG) was purchased from Sigma-Aldrich (St. Louis, MO). PEG was dissolved in 10 mM PBS to a concentration of 0.1 mg/ml and prepared fresh for each test. Bovine serum albumin (BSA) from Sigma–Aldrich (St. Louis, MO, USA) was prepared in PBS (1.0%, w/v) as an alternative blocking solution. Streptavidin was purchased from Rockland Inc. (Gilbertsville, PA). It was reconstituted in 10 mM PBS and stored in 1 mg/ml aliquots at -20 °C. The streptavidin was diluted to 0.25 mg/ml for use in tests. All water used in tests was obtained from a Millipore water purification system (Mill-Q, Bedford, MA).

### **4.1.2 Virus and Aptamers**

Inactivated avian influenza A/H5N1 virus was obtained from the USDA/National Veterinary Services Laboratory in Ames, Iowa. The virus was inactivated by the USDA lab using  $\beta$ -propiolactone. The H5N1 virus used in the tests was isolated from chickens in Scotland in 1959. The stock concentration of the virus was 128 Hemagglutination unit/50  $\mu$ l (HAU). All dilutions were done using PBS. Killed AIV H7N2, H9N2, H5N9, H5N2, and H5N3 were obtained from Animal Diagnostic Laboratory at Penn State University, University Park, PA. Subtypes were picked for overlapping antigenic properties with AIV H5N1.

The H5N1 aptamer was previously developed in our laboratory through the SELEX method (Wang & Li, 2013), and the sequence is as follows:

5'-GTGTGCATGGATAGCACGTAACGGTGTAGTAGATACGTGCGGGTAGGAAGAAAG  
GGAAATAGTTGTCCTGTTG-3'

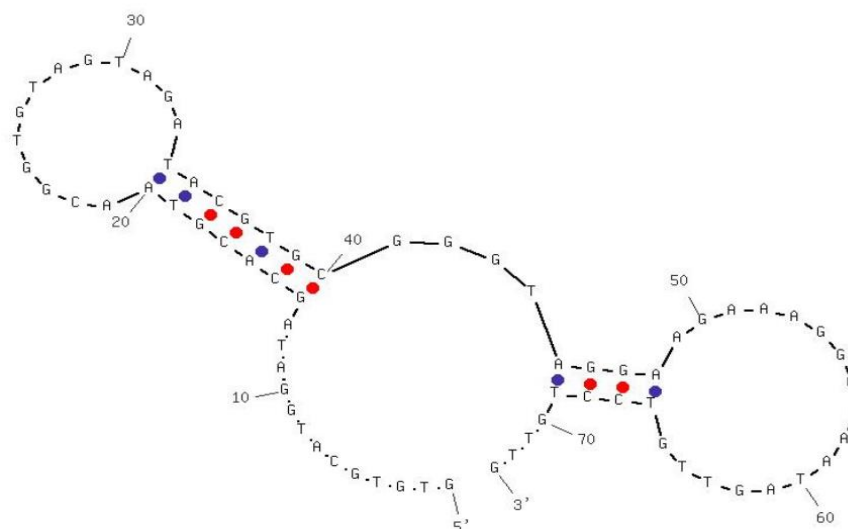


**Figure 4.1-** H5N1 aptamer secondary structure (from Wang & Li, 2013)

The aptamer was synthesized and biotin labeled by Integrated DNA Technologies (Coralville, IA). The aptamer was aliquoted and stored at -20 °C. The aliquots were diluted using PBS to a working concentration of 0.023 mg/ml (1  $\mu$ M).

#### 4.1.3 Instruments and Electrodes

Figure 4.2 shows the general aptasensor set up. All measurements were taken with the QCA 922 Quartz Crystal Analyzer from Princeton Applied Research (Oak Ridge, TN) with the WinEchem software used to collect and plot the data. The leads of the QCM were connected to the electrode and frequency and resistance measurements were taken at 1 s intervals. All measurements were done in PBS at room temperature.

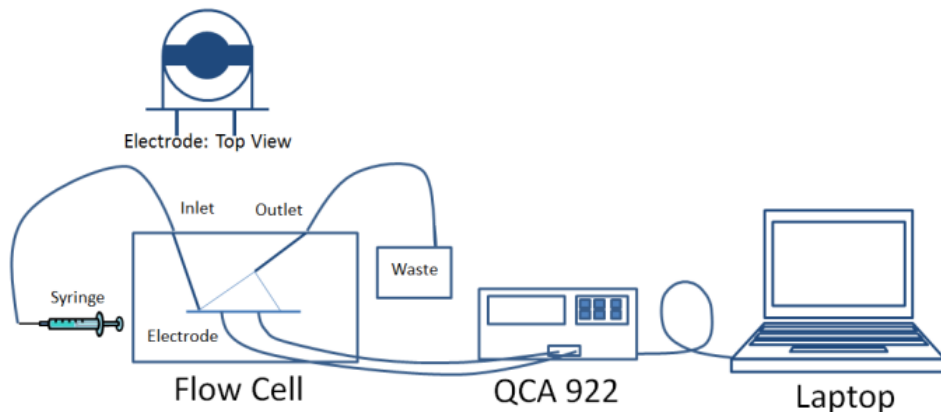


**Figure 4.2** - Schematic of the aptasensor. The biological sensing element is immobilized on the electrode surface. The quartz in the electrode acts as a transducer, converting the mass change to a frequency signal. The QCM processes and records all of the data.

AT-cut quartz crystals (13.7 mm diameter) were obtained from International Crystal Manufacturing (Oklahoma City, OK). The crystals had a resonant frequency of 7.995 MHz, and its surface was polished with gold (5.1 mm diameter).

A flow cell from International Crystal Manufacturing (Oklahoma City, OK) was used for mounting the crystal electrode and holding the testing sample. The two flow cell pieces were screwed together to hold the electrode in place and was sealed with two O-rings. A 70  $\mu$ l chamber was located above the polished gold surface for the injection of the testing samples.

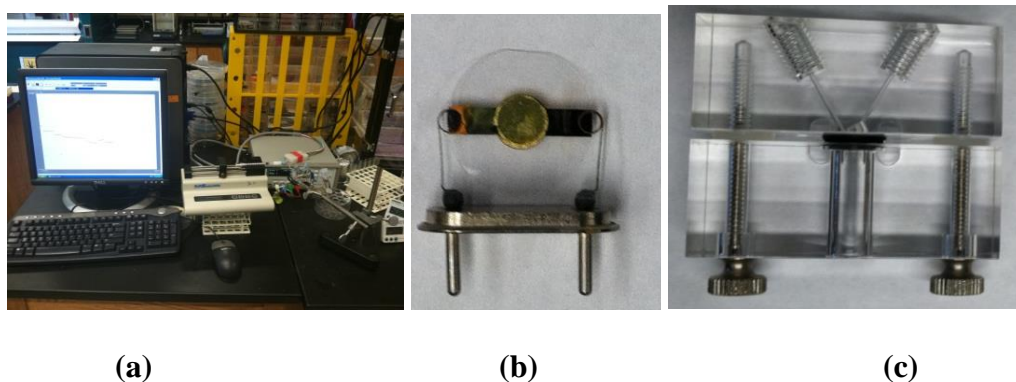


**Figure 4.3-** Instruments and electrodes. (a) QCA 922 quartz crystal analyzer. (b) 8 MHz AT-cut quartz crystal electrode. (c) 70  $\mu$ l acrylic flow cell.

## **4.2 Detection of AIV H5N1**

### **4.2.1 Pretreatment of Electrodes**

The crystal's electrodes were first cleaned by immersing them in 1 M NaOH for 20 min. Then a freshly prepared piranha solution (1:3 H<sub>2</sub>O<sub>2</sub>:H<sub>2</sub>SO<sub>4</sub>) was dropped on the gold surface for 1 min. Special care was taken to keep this solution away from the electrode leads. The electrodes were washed with deionized water and dried in a stream of nitrogen after each pretreatment. The crystal was then ready for installation into the flow cell.

### **4.2.2 Preparation of 150 nm Magnetic Nanobeads**

MagCelect Streptavidin Ferrofluid nanobeads with a diameter of 150 nm were obtained from R&D systems (Minneapolis, MN) and used at stock concentration. The MagCelect Streptavidin Ferrofluid was a colloid of magnetic nanoparticles conjugated to streptavidin in solution containing Bovine Serum Albumin (BSA) and preservatives.

A 20 µl streptavidin coated nanobead solution was mixed with 200 µl of PBS and then a magnetic field at 0.8 T was applied for 2 min using a magnetic separator (AIBIT LLC., Jiangyin, China). The nanobeads were then resuspended in 100 µl of aptamers and 100 µl of PBS. The solution was rotated at 15 rpm for 30 min. Next, the nanobeads were suspended in 100 µl of PBS and 100 µl of biotin solution and rotated again for 10 min. After each step the magnetic separation and washing was repeated, resuspending the nanobeads in 200 µl of PBS.

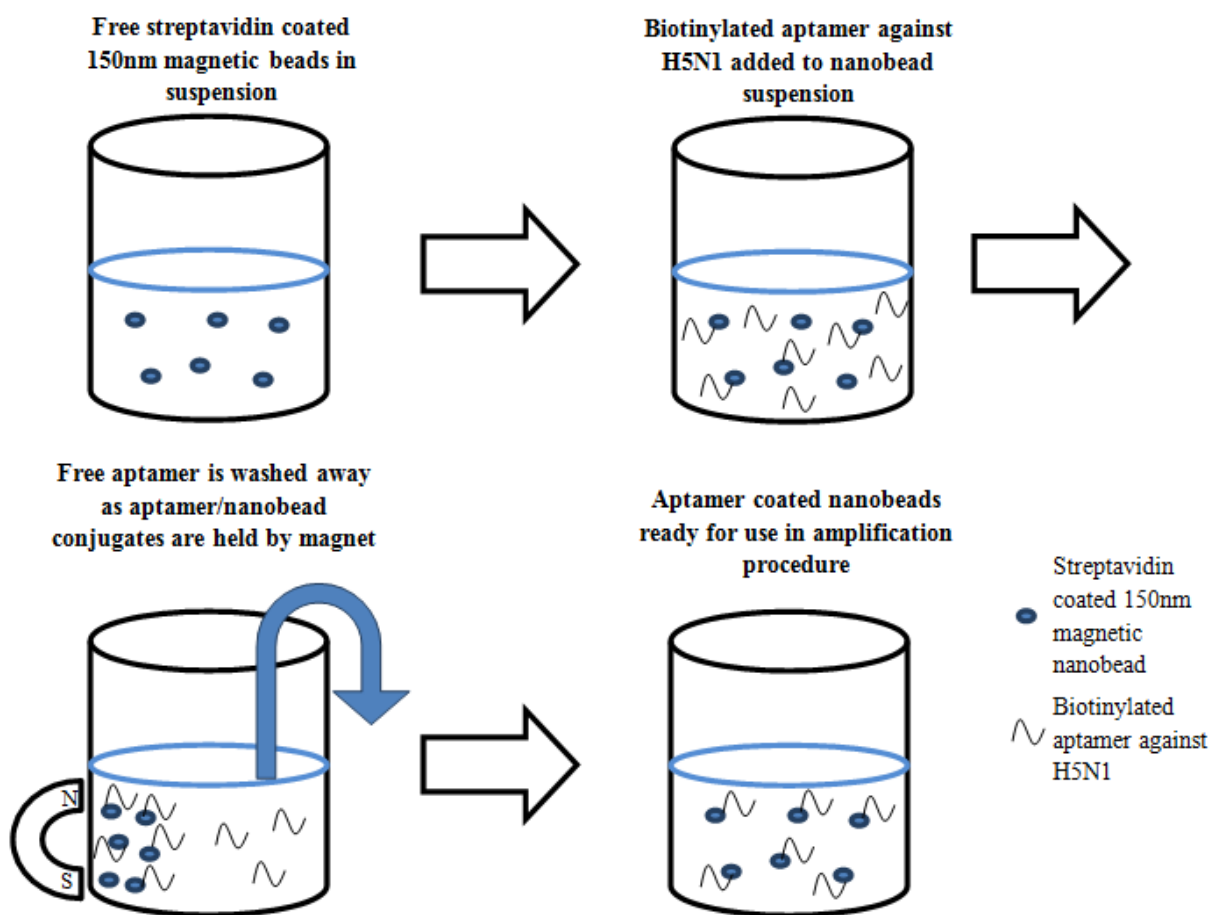
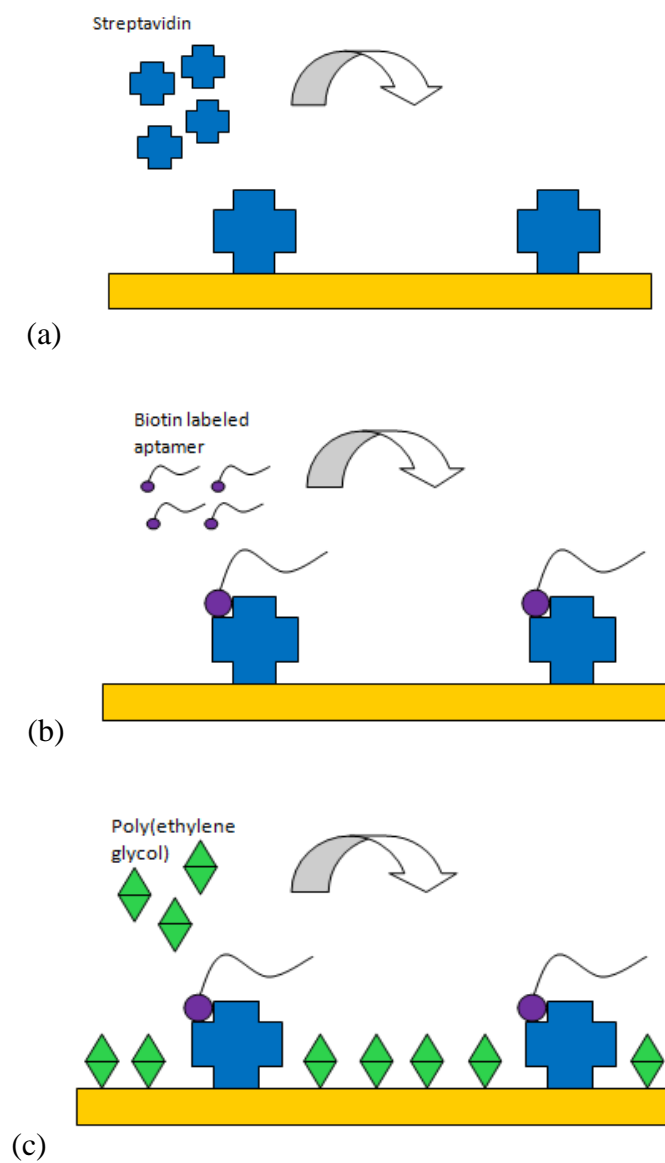


**Figure 4.4-** Functionalization of streptavidin coated 150 nm magnetic nanobeads with biotinylated aptamer against H5N1

### 4.2.3 Detection of AIV H5N1

A schematic of the electrode pretreatment and aptamer immobilization is shown in figure 4.5 a, b, and c. PBS solution was first injected into the flow cell to provide a baseline measurement. Streptavidin (0.25 mg/ml) was then added to the flow cell for 30 min and allowed to bind to the electrode surface through protein adsorption. Biotin labeled H5N1 aptamer (1  $\mu$ M) was injected into the flow cell and allowed to incubate for 15 min. Next, poly(ethylene glycol) methyl ether thiol (0.1 mg/ml) was added for 1 h to prevent any nonspecific binding to the

electrode surface. Before the use of PEG, BSA was tested as a blocking agent. 1% BSA was injected and allowed to incubate for 20 min. Inactivated AIV H5N1 with titers in the range of 0.01-4 HAU/50  $\mu$ l in PBS were added to the flow cell for capturing by the aptamer immobilized on the surface of QCM sensor and allowed to incubate for 30 min (figure 4.5 d). All uses of HAU refer to HAU/50  $\mu$ l. Next, the aptamer coated nanobeads were injected into the flow cell for 30 min to allow binding to the captured virus (figure 4.5 e).



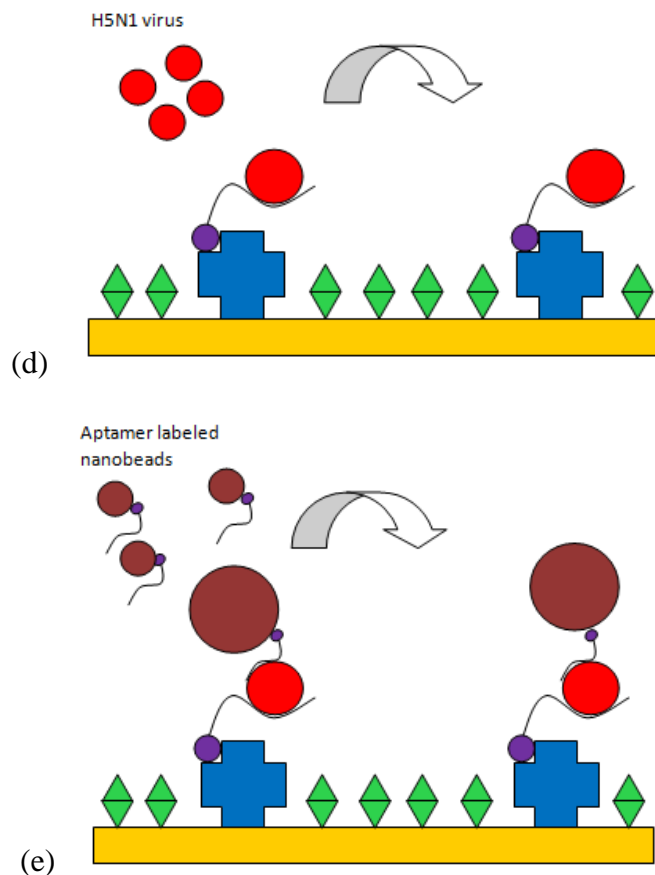


**Figure 4.5-** The electrode modification, virus detection and signal amplification of the aptasensor. a) Streptavidin adsorption; b) aptamer immobilization by streptavidin binding; c) PEG blocking of unbound sites; d) capturing of target H5N1 virus; e) amplification by nanobead labeling.

#### 4.2.4 Specificity Tests

Specificity tests were conducted using inactivated AIV H7N2, H9N2, H5N9, H5N2, and H5N3 subtypes at 2 HAU. These were chosen because of their overlapping antigenic properties with H5N1. Triplicate tests were run at this concentration to determine the aptasensor's sensitivity and specificity to non-target viruses.

#### 4.2.5 Data Analysis

The mean and standard deviation of frequency changes were calculated and plotted using Microsoft Excel. The threshold for positive detection or lower detection limit was set as signal/noise ratio of 3 where the noise is defined as the standard deviation of the control sample. JMP was used for all statistical analysis. Analysis of variance (ANOVA) was used to calculate the P values of each of the treatments comparing the frequency changes before and after nanobead amplification.

### 4.3 Calculation of Captured Virus

Using our measured frequency values along with the equations suggested in the literature review the approximate number of target virus particles captured by the aptasensor could be calculated. Equation 3.2 reflects the changes made to the frequency due to a liquid solution being present. Because we focused on the change in frequency before and after the addition of AIV H5N1, the liquid portion of the equation could be cancelled out due to both measurements being taken in a PBS solution. Thus, equation 3.1 was used to calculate the number of virus particles captured based on the measured frequency changes for each titer. Assuming an average size of 80 nm and a density of 1.1 g/cm<sup>3</sup> (Kahler & Lloyd, 1951) the calculated change in mass could be converted to an actual number of virus particles captured.

The values and units for each term in equation 3.1 are as follows:  $\Delta f$  = measured value (Hz),  $C_f = 2.3 \times 10^{-6}$  (cm<sup>2</sup>/g·Hz),  $f_0 = 8$  (MHz),  $\Delta m$  = mass of virus captured (g),  $A = .196$  (cm<sup>2</sup>).

The number of virus particles captured was estimated by using the equation:

$$N = \frac{\Delta m}{(\rho \cdot V)} \quad 4.1$$

where  $N$  is the number of virus particles,  $\rho$  is the density of the virus in g/cm<sup>3</sup>, and  $V$  is the volume of one virus particle in cm<sup>3</sup>.



## **Chapter 5 Results and Discussion**

## 5.1 Fabrication and Characterization of the QCM Aptasensor

As shown in Figure 4.5, the experiments were conducted by following the stepwise fabrication and detection of the QCM biosensor, including target binding and signal amplification. Initial tests were run with no blocking agent prior to the addition of H5N1 virus and magnetic nanobeads. Negative control tests showed a significant amount of non-specific binding of the virus and nanobeads to the gold surface in the absence of aptamers. The first solution was to use Bovine Serum Albumin (BSA) to block the remaining free gold surface from any non-specific binding. However, this was found to also inhibit the capturing of the target virus by the aptamer, most likely due to the large size of BSA ( $\approx 12$  nm) relative to the aptamer size ( $\approx 3$  nm). Poly(ethylene glycol) methyl ether thiol (PEG) was then used due to its small size and strong blocking capabilities. PEG proved to be very effective for not only preventing non-specific binding to the gold surface but also not interfering with the aptamer's ability to capture the target virus. Figure 5.1 shows a comparison of the two blocking agents. BSA blocking actually caused a decrease in mass after the addition of AIV H5N1 virus at 4 HAU, most likely due to the BSA being washed away easily from the shear stress of the fluid flow. PEG clearly allows the aptamer to still capture the target virus. The target H5N1 virus was then added to the flow cell and would bind to the immobilized aptamer. Lastly, 150 nm magnetic nanobeads modified with the H5N1 aptamer were used as biolabels for further amplifying the mass of the virus particles. Each of these steps caused a decrease in the resonant frequency of the electrode due to an increase in mass. The net response from each step is determined by the difference in the corresponding PBS baselines.



**Figure 5.1-** Frequency shifts of the QCM aptasensor comparing BSA and PEG blocking agents for AIV H5N1.

Figure 5.2 shows a typical sensorgram of virus detection with the aptasensor. The adsorption of streptavidin to the gold surface along with the immobilization of the aptamer were both verified in real time by the decreases in frequency, 77 Hz and 46 Hz respectively. PEG required a long binding time of 1 h in order to completely block the remaining electrode surface and further decreased the frequency by 2 Hz. Following the blocking step, the target virus was captured by the aptamer and caused a 44 Hz decrease in frequency. Lastly, nanobead amplification further increased the frequency change by 10 Hz by binding to the H5N1 virus. Each step was followed by a PBS washing step to wash away any unbound materials and to create a stable baseline prior to the next injection.

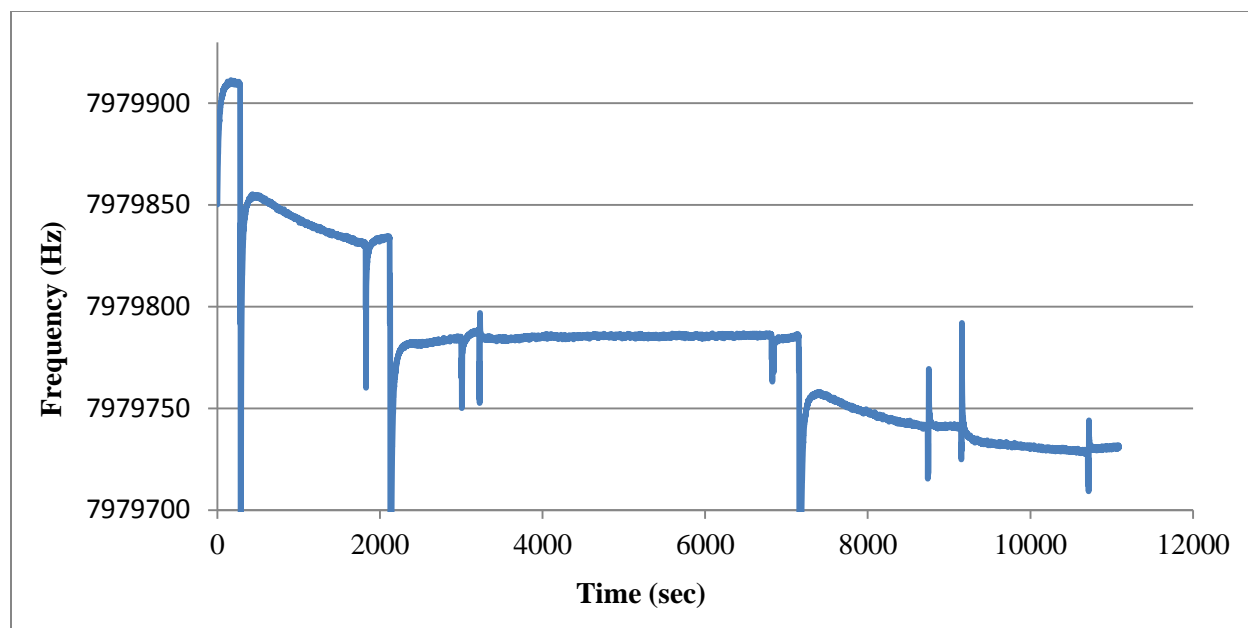


**Figure 5.2-** Typical sensorgram of the QCM aptasensor for surface modification, aptamer immobilization, target AIV detection and signal amplification with nanobeads. The concentration of AIV H5N1 was 1 HA in this test.

## 5.2 Detection of AIV H5N1

The total detection time for the detection of virus and amplification with nanobeads is 1 h for this sensor. The detection signal was the change in frequency of the PBS baselines due to the addition of the virus and nanobeads and the results can be seen in figure 5.3. The threshold for positive detection was set as 3 x noise (addition of nanobeads with no virus present). The detection limit of this sensor was determined to be 1 HAU. Using the same calculation method, the detection limit of the biosensor was also 1 HAU for H5N1 detection without nanobead amplification.

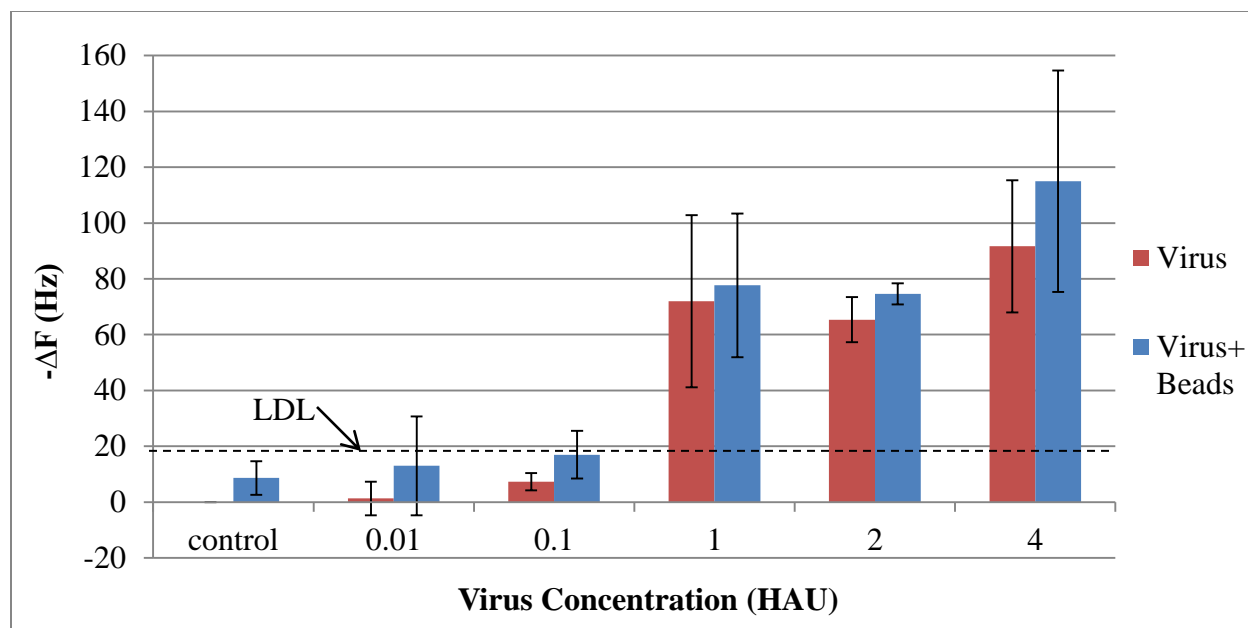


**Figure 5.3-** Frequency shifts of the QCM aptasensor as a function of the titer (HAU) of AI H5N1 virus in PBS solution. The detection limit is determined as 1 HAU. Error bars indicate the standard deviation (n=3).

Table 1 presents the detailed frequency shifts of the QCM aptasensor caused by the capturing of the target H5N1 virus along with the amplification by 150 nm magnetic nanobeads.

**Table 5.1-** Frequency values of the QCM aptasensor for each titer (HAU) of AI H5N1 virus in PBS solution. Error values indicate the standard deviation (n=3).

Titers of H5N1 Virus (HA unit)	Frequency Shift (-ΔF (Hz) ± S.D.)	
	Virus	Virus+Nanobeads
4	92 ± 24	115 ± 40
2	65 ± 8	75 ± 4
1	72 ± 31	78 ± 26
0.1	7 ± 3	17 ± 9
0.01	1 ± 6	13 ± 18
Control	0 ± 0	9 ± 6

Table 5.2 shows the calculated virus numbers for each titer. The numbers show that more virus particles were potentially captured than that was added in to the system. This could possibly be explained by the presence of other impurities that would settle on the electrode surface. Also, there might be a small change in the viscoelastic properties of the solution which would have some effect on the frequency measurements.

**Table 5.2-** Comparison of calculated virus capture versus the number of virus added.

Titers of H5N1 Virus (HA unit)	$-\Delta F$ (Hz)	No. of Virus Captured	No. of Virus Added
4	92	4.15E+08	2.00E+08
2	65	2.93E+08	1.00E+08
1	72	3.25E+08	5.00E+07
0.1	7	3.31E+07	5.00E+06
0.01	1	6.02E+06	5.00E+05

JMP was used to perform statistical analysis of the data collected. Table 5.3 compares each of the treatments (titers) to determine which are significantly different from each other. The results are pretty expected. The concentrations below the detection limit all came back as not significantly different from one another because the aptasensor was not sensitive enough to detect them.

**Table 5.3-** Comparison of treatment means. Levels not connected by the same letter are not significantly different.

Levels		Least Sq Mean
4	A	103.33333
1	B	74.83333
2	B	70.00000
0.1	C	12.16667
0.01	C	7.16667
0	C	4.33333

In addition to comparing treatment values, the means of the virus and virus+beads values were compared to determine whether the addition of beads was significant in increasing the sensitivity of the sensor. The P value for each concentration was determined using ANOVA analysis in JMP. P values greater than our alpha ( $\alpha=.05$ ) are considered not significantly different. Table 5.4 shows that the nanobead amplification was insignificant for all concentrations of virus.

**Table 5.4-** P values for each H5N1 concentration determining the significance of nanobead amplification. P values greater than .05 are considered not significantly different.

Concentration	P value
4	0.4311
2	0.1444
1	0.8188
0.1	0.1388
0.01	0.3405
control	0.0675

Compared to the QCM immunosensor reported by Li et al. (2011), the aptamer seemed to be much more effective in the capturing virus than the more commonly used antibody. Not only was the magnitude of the frequency change higher for each respective titer, but the aptamer also cut the detection time in half compared to antibody tests. Also, the aptamers did not require chemical immobilization which is time consuming and material intensive. However, the aptamer coated nanobeads were not as effective as a mass amplifier as hoped. While they did slightly increase the sensitivity of the biosensor, this was not enough to lower the detection limit from the pure virus detection limit. It should be noted that as the titer concentration lowered, the bead amplification became more and more significant. At 0.1 and 0.01 HAU the nanobeads more than doubled the frequency change due to the capture of AIV H5N1. Unfortunately, this was still below the lower detection limit of the aptasensor. If the noise level could be lowered by further reducing nonspecific binding of nanobeads the aptasensor would prove to be even more sensitive. A possible explanation for the failure of the nanobead amplification could be the non-rigid structure of the AIV/nanobead complex. The QCM is much more sensitive to rigid structures compared to elastic ones. Antibodies provide a more rigid structure and can bind to multiple virus particles as well while aptamers are more flexible and only have one binding site. While aptamers are still great for very specific virus detection, they are not as strong when it comes to nanobead amplification because of the elasticity of their structure.

Figure 5.4 shows an SEM image of the top of the QCM electrode surface. The image confirms the capturing of the target H5N1 virus by the aptamer and also the binding of the 150 nm magnetic nanobead to the virus.



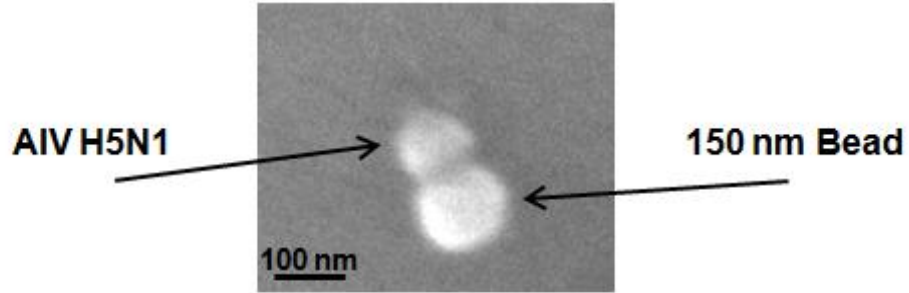


**Figure 5.4-** SEM image of the top view of the QCM surface. Confirmation of the binding of a magnetic nanobead with a 150 nm diameter to a target H5N1 virus (80 nm diameter).

### 5.3 Specificity of the Aptasensor

The aptasensor was evaluated for specificity with five different subtypes of avian influenza viruses using the same procedure described previously. These non-target viruses were chosen due to the similar properties of their HA and NA proteins. Figure 5.5 shows the frequency change due to the addition of each non-target virus at a concentration of 2 HAU. While AIV H5N1 made 65 Hz of frequency change, none of the five non-target subtypes caused more than 8 Hz of frequency change, which is well below the lower detection limit of 18 Hz frequency change. The results proved a high specificity of the aptasensor to the target AIV H5N1. One thing of note is that the calculation of the lower detection limit should have been adjusted for the specificity tests. The original LDL was determined using a negative control with nanobeads. That should not apply to this case because nanobeads were not used in this part of the experiment. Therefore, a baseline of PBS should have been measured for 30 min. Taking three times the standard deviation of the PBS frequency change would give a more accurate determination of the lower detection limit for the specificity tests.

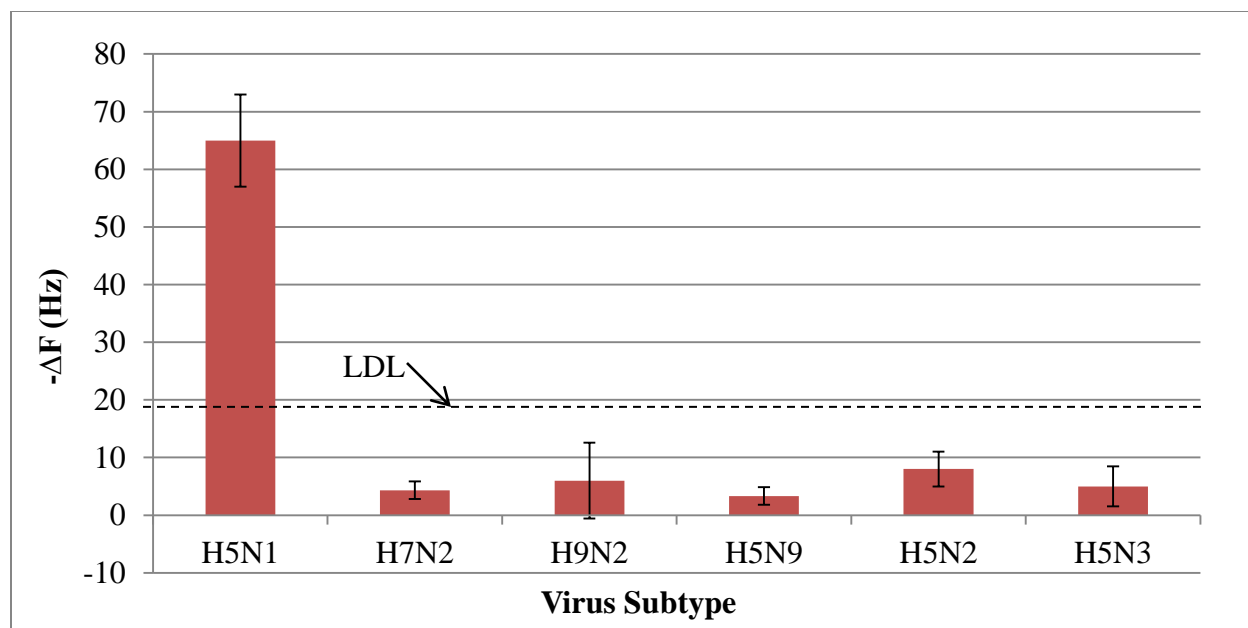


**Figure 5.5-** Frequency shifts of the QCM aptasensor for the target AIV H5N1 virus along with the five non-target AIV subtypes at 2 HAU. Error bars indicate standard deviation (n=3).

## **Chapter 6    Conclusions**

A QCM aptasensor was designed and fabricated for rapid detection of avian influenza virus. Experiments were completed to determine the effectiveness of aptamers as a biological recognition element as well as magnetic nanobeads as mass amplifiers in order to improve the sensitivity and specificity of the AIV H5N1 biosensor. The results of this study showed that the aptamer not only increased the specificity of the aptasensor to the target virus but also reduced the detection time, compared with the immunosensor developed by Li et al. (2011). A detection limit of 1 HAU was determined for AIV H5N1. Unfortunately, the nanobead amplification proved to be insignificant by not amplifying the frequency change enough to lower the detection limit. If the noise level could be reduced the sensor's sensitivity could be greatly increased since the nanobead significantly increased the signal when the concentration of AIV was low. While the detection limit of this aptasensor was very similar to previous studies (1 HAU), it has the advantage of being specific to the H5N1 virus rather than just the H5 protein. The aptasensor was proven to have no non-specific binding to similar non-target AIV subtypes. The detection time of the aptasensor was also greatly reduced down to 1 h.

## **Chapter 7    Recommendations for Future Research**

Further improvements of the biosensor could be accomplished by addressing the issue of the nanobead amplification. More testing could be done using several types of nanoparticles to determine which one is the optimal choice for QCM and virus labeling. The colloid beads were not very effective in binding to the target virus which could have been caused by their random shape. A more uniform nanobead could be much more effective. Also trying nanowire and nanotubes along with different sizes of nanobeads could prove to be beneficial in determining the best amplification agent.

## References

- Amano, Y., & Cheng, Q. (2005). Detection of influenza virus: Traditional approaches and development of biosensors. *Anal. Bioanal. Chem.* 381(1), 156-164.
- Bai, H., Wang, R., Hargis, B., Lu, H., & Li, Y. (2012). A SPR aptasensor for detection of avian influenza virus H5N1. *Sensors* 12(9), 12506-12518.
- Balamurugan, S., Obubuafo, A., Soper, S. A., & Spivak, D. A. (2007). Surface immobilization methods for aptamer diagnostic applications. *Anal. Bioanal. Chem.* 390(1), 1009-1021.
- Bard, A. J., & Faulkner, L.R. (2001). *Electrochemical Methods: Fundamentals and Applications*. 2nd Edition. John Wiley & Sons. New York.
- Boyce, W. M., Sandrock, C., Kreuder-Johnson, C., Kelly, T., & Cardona, C. (2009). Avian influenza viruses in wild birds: A moving target. *Comp. Immunol. Microbiol. Infect. Dis.* 32(4), 275-286.
- Burns, A., van der Mensbrugge, & D., Timmer, H. (2008). Evaluating the economic consequences of avian influenza. World Bank report. [http://siteresources.worldbank.org/EXTAVIANFLU/Resources/EvaluatingAHIeconomic\\_s\\_2008.pdf](http://siteresources.worldbank.org/EXTAVIANFLU/Resources/EvaluatingAHIeconomic_s_2008.pdf). Accessed September 12, 2012.
- Chang, Y., Wang, S., Huang, J.C., Su, L., Yao, L., Li, Y. et al. (2010). Detection of swine-origin influenza A (H1N1) viruses using a localized surface plasmon coupled fluorescence fiber-optic biosensor. *Biosens. Bioelectron.* 26(3), 1068-1073.
- Charlton, B., Crossley, B., & Hietala, S. (2009). Conventional and future diagnostics for avian influenza. *Comp. Immunol. Microbiol. Infect. Dis.* 32(4), 341-350.
- Cooper, M. A. (2002). Optical biosensors in drug discovery. *Nat. Rev. Drug Discov.* 1(7), 515-528.
- Cui, Z., Ren, Q., Wei, H., Chen, Z., Deng, J., et al. (2011). Quantum dot-aptamer nanoprobe for recognizing and labeling influenza A virus particles. *Nanoscale* 3(1), 2454-2457.
- Davis, F., & Higson, S. P. (2010). Label-free immunochemistry approach to detect and identify antibiotics in milk. *Pediatr. Rev.* 67(5), 476-480.
- Dawson, E. D., Moore, C. L., Dankbar, D. M., Mehlmann, M., Townsend, M. B., Smagala, J. A., et al. (2007). Identification of A/H5N1 influenza viruses using a single gene diagnostic microarray. *Anal. Chem.* 79(1), 378-384.
- Deisingh, A. K., & Thompson, M. (2004). Biosensors for the detection of bacteria. *Can. J. Microbiol.* 50(2), 69-77.

- Ellington, A.D., & Szostak, J.W.. (1990). In vitro selection of RNA molecules that bind specific ligands. *Nature* 346(6287), 818-822.
- Ellis, J. S., & Zambon, M. C. (2002). Molecular diagnosis of influenza. *Rev. Med. Virol.* 12(6), 375-389.
- Estmer-Nilsson, C., Abbas, S., Bennemo, M., Larsson, A., Hämäläinen, M. D., & Frostell-Karlsson, Å. (2010). A novel assay for influenza virus quantification using surface plasmon resonance. *Vaccine* 28(3), 759-766.
- Fang, L. Q., de Vlas, S. J., Liang, S., Looman, C. W., Gong, P., Xu, B., et al. (2008). Environmental factors contributing to the spread of H5N1 avian influenza in mainland china. *PloS One* 3(5), e2268.
- Fortineau, N., Trieu-Cuot, P., Gaillot, O., Pellegrini, E., Berche, P., & Gaillard, J. (2000). Optimization of green fluorescent protein expression vectors for in vitro and in vivo detection of listeria monocytogenes. *Res. Microbiol.* 151(5), 353-360.
- Grieshaber, D., MacKenzie, R., Vörös, J., & Reimhult, E. (2008). Electrochemical biosensors - sensor principles and architectures. *Sensors* 8(3), 1400-1458.
- Harder, T.C., & Werner, O. (2006). Avian influenza. Influenza report. <http://www.influenzareport.com/ir/ai.htm>. Accessed September 18, 2012.
- Hien, N. D., Ha, N. H., Van, N. T., Ha, N. T., Lien, T. T., Thai, N. Q., et al. (2009). Human infection with highly pathogenic avian influenza virus (H5N1) in northern vietnam, 2004-2005. *Emerg. Infect. Diseases* 15(1), 19-23.
- Hsing, I., Xu, Y., & Zhao, W. (2007). Micro- and nano- magnetic particles for applications in biosensing. *Electroanal.* 19(7-8), 755-768.
- Ivnitski, D., Abdel-Hamid, I., Atanasov, P., & Wilkins, E. (1999). Biosensors for detection of pathogenic bacteria. *Biosens. Bioelectron.* 14(7), 599-624.
- Jayasena, S.D. (1999). Aptamers: An emerging class of molecules that rival antibodies in diagnostics. *Clin. Chem.* 45(9), 1628-1650.
- Jenison, R.D., Gill, S.C., Pardi A., & Polisky, B. (1994). High-resolution molecular discrimination by RNA. *Science* 263(5152), 1425-1429.
- Jin, H., Leser, G. P., Zhang, J., & Lamb, R. A. (1997). Influenza virus hemagglutinin and neuraminidase cytoplasmic tails control particle shape. *EMBO J.* 16(6), 1236-1247.
- Kahler, H., & Lloyd Jr., B.J. (1951). Density of polystyrenelatex by a centrifugal method. *Science* 114(1), 34-35.



- Kamikawa, T. L., Mikolajczyk, M. G., Kennedy, M., Zhang, P., Wang, W., Scott, D. E. et al. (2012). Nanoparticle-based biosensor for the detection of emerging pandemic influenza strains. *Biosens. Bioelectron.* 26(4), 1346-1352.
- Kanazawa, K.K., & Gordon, J.G. (1985). The oscillation frequency of a quartz resonator in contact with liquid. *Anal. Chim. Acta* 175(1), 99-105.
- Koncki, R. (2007). Recent developments in potentiometric biosensors for biomedical analysis. *Anal. Chim. Acta* 599(1), 7-15.
- Lee, C., & Saif, Y. M. (2009). Avian influenza virus. *Comp. Immunol. Microbiol. Infect. Dis.* 32(4), 301-310.
- Leland, D. S., & Ginocchio, C. C. (2007). Role of cell culture for virus detection in the age of technology. *Clin. Microbiol. Rev.* 20(1), 49-78.
- Li, D., Wang, J., Wang, R., Li, Y., Abi-Ghanem, D., Berghman, L., Hargis, B. & Lu, H. (2011). A nanobeads amplified QCM immunosensor for the detection of avian influenza virus H5N1. *Biosens. Bioelectron.* 26(1), 4146-4154.
- Li, K. S., Guan, Y., Wang, J., Smith, G. J., Xu, K. M., Duan, L., et al. (2004). Genesis of a highly pathogenic and potentially pandemic H5N1 influenza virus in eastern asia. *Nature* 430(6996), 209-213.
- Liu, F., Li, Y., Su, X., Slavik, M.F., Ying, Y., & Wang, J. (2007). QCM immunosensor with nanoparticle amplification for detection of Escherichia coli O157:H7. *Sens. Instrumen. Food Qual.* 1(1), 161-168.
- Lojou, E., & Bianco, P. (2006). Application of the electrochemical concepts and techniques to amperometric biosensor devices. *J. Electroceram.* 16(1), 79-91.
- Lu, C., & Czanderna, A. W. (1984). *Methods and Phenomena 7: Applications of Piezoelectric Quartz Crystal Microbalance*. Volume 7. Elsevier. Amsterdam.
- Lum, J., Wang, R., Lassiter, K., Srinivasan, B., Abi-Ghanem, D., Berghman, L. et al. (2012). Rapid detection of avian influenza H5N1 virus using impedance measurement of immuno-reaction coupled with RBC amplification. *Biosens. Bioelectron.* 38(1), 67-73.
- Marandi, V. (2010). Assesment of a rapid immunochromatographic assay for the detection of avian influenza viruses. *Int. J. Vet. Res.* 4(3), 183-188.
- Mascini, M. (2009). *Aptamers in Bioanalysis*. John Wiley & Sons. Chichester.
- Medintz, I. L., Uyeda, H. T., Goldman, E. R., & Mattoussi, H. (2005). Quantum dot bioconjugates for imaging, labelling and sensing. *Nature Mat.* 4(6), 435-446.

- Mitnaul, L. J., Matrosovich, M. N., Castrucci, M. R., Tuzikov, A. B., Bovin, N. V., Kobasa, D., et al. (2000). Balanced hemagglutinin and neuraminidase activities are critical for efficient replication of influenza A virus. *J. Virol.* 74(13), 6015-6020.
- Nayak, M., Kotian, A., Marathe, S., & Chakravorty, D. (2009). Detection of microorganisms using biosensors—A smarter way towards detection techniques. *Biosens. Bioelectron.* 25(4), 661-667.
- Nguyen, T. N., Ung, T. D., Vu, T. H., Tran, T. K., Dong, V. Q., Dinh, D. K. et al. (2012). Fluorescence biosensor based on CdTe quantum dots for specific detection of H5N1 avian influenza virus. *Adv. Nat. Sci: Nanosci. Nanotechnol.* 3(035014), 5 pp.
- Owen, T.W., Al-Kaysi, R.O., Bardeen, C.J. & Cheng, Q. (2007). Microgravimetric immunosensor for direct detection of aerosolized influenza A virus particles. *Sensors and Actuators B* 126(1), 691-699.
- Peduru Hewa, T. M., Tannock, G. A., Mainwaring, D. E., Harrison, S., & Fecondo, J. V. (2009). The detection of influenza A and B viruses in clinical specimens using a quartz crystal microbalance. *J. Virol. Meth.* 162(1-2), 14-21.
- Pejcic, B., De Marco, R., & Parkinson, G. (2006). The role of biosensors in the detection of emerging infectious diseases. *Analyst* 131(10), 1079-1090.
- Phillips, K. S., & Cheng, Q. (2007). Recent advances in surface plasmon resonance based techniques for bioanalysis. *Anal. Bioanal. Chem.* 387(5), 1831-1840.
- Sauerbrey, G. (1959). Verwendung von schwingquarzen zur wägung dünner schichten und zur mikorwägung. *Zeitschrift für Physik* 155(1), 206-222
- Sefah, K., Phillips, J.A., Xiong, X., Meng, L., Van Simaey, D., Chen, H. et al. 2009. Nucleic acid aptamers for biosensors and bio-analytical applications. *Analyst* 134(1), 1765-1775.
- Steinhauer, D. A. (1999). Role of hemagglutinin cleavage for the pathogenicity of influenza virus. *J. Virol.* 258(1), 1-20.
- Thorson, A., Petzold, M., Nguyen, T. K., & Ekdahl, K. (2006). Is exposure to sick or dead poultry associated with flulike illness?: A population-based study from a rural area in vietnam with outbreaks of highly pathogenic avian influenza. *Arch. Intern. Med.* 166(1), 119-123.
- Tsai, H., Lin, Y., Chang, H. W., & Fuh, C. B. (2008). Integrating the QCM detection with magnetic separation for on-line analysis. *Biosens. Bioelectron.* 24(3), 485-488.
- Tuerk, C., & Gold, L. (1990). Systematic evolution of ligands by exponential enrichment: RNA ligands to bacteriophage T4 DNA polymerase. *Science* 249(4968), 505-510.

- Varshney, M., & Li, Y. (2009). Interdigitated array microelectrodes based impedance biosensors for detection of bacterial cells. *Biosens. Bioelectron.* 24(10), 2951-2960.
- Vogt, B. D., Lin, E. K., Wu, W., & White, C. C. (2004). Effect of film thickness on the validity of the sauerbrey equation for hydrated polyelectrolyte films. *J. Phys. Chem. B* 108(1), 12685-12690.
- Wang, J. (2001). Glucose biosensors: 40 years of advances and challenges. *Electroanal.* 13(12), 983-988.
- Wang, J. (2006). Electrochemical biosensors: Towards point-of-care cancer diagnostics. *Biosens. Bioelectron.* 21(10), 1887-1892.
- Wang, J. (2008). Electrochemical glucose biosensors. *Chem. Rev.* 108(2), 814-825.
- Wang, R., & Li, Y. (2013). Hydrogel based QCM aptasensor for detection of avian influenza virus," *Biosens. Bioelectron.* 42(1), 148-155.
- Wang, R., Wang, Y., Lassiter, K., Li, Y., Hargis, B., Tung, S., et al. (2009). Interdigitated array microelectrode based impedance immunosensor for detection of avian influenza virus H5N1. *Talanta* 79(2), 159-164.
- WHO. (2013). Cumulative Number of Confirmed Human Cases of Avian Influenza A/(H5N1) Reported to WHO, 2003-2013. [http://www.who.int/influenza/human\\_animal\\_interface/EN\\_GIP\\_20130312CumulativeNumberH5N1cases.pdf](http://www.who.int/influenza/human_animal_interface/EN_GIP_20130312CumulativeNumberH5N1cases.pdf). Accessed July 22, 2010.
- Xu, J., Suarez, D., & Gottfried, D.S. (2007). Detection of avian influenza virus using an interferometric biosensor," *Anal. Bioanal. Chem.* 389(1), 1193-1199.
- Yang, L., & Li, Y. (2006). Detection of viable salmonella using microelectrode-based capacitance measurement coupled with immunomagnetic separation. *J. Microbiol. Meth.* 64(1), 9-16.